

THE STRUCTURAL AND PIEZOELECTRIC
PROPERTIES OF EPITAXIAL A&N ON Al_2O_3 *

F. A. Pizzarello and J. E. Coker

Rockwell International
Autonetics Group
Electronics Research Division
3370 Miraloma Avenue
Anaheim, California 92803

(Received May 6, 1974; revised August 23, 1974)

The piezoelectric properties of epitaxial A&N films grown by the method of chemical vapor deposition utilizing trimethylaluminum and ammonia as chemical reactants were investigated. Large variations of the measured electro-mechanical coupling coefficient, k^2 , were found in different regions of the same sample and on different samples having approximately the same h/λ value. Electron microscope observations of replicated as-grown and etched surfaces of epitaxial A&N were used to show a relationship between surface facet ordering and the magnitude of k^2 . A plot of k^2 measured at various h/λ values shows k^2 as large as 0.6% for films grown at a rate of $\sim 0.2 \mu\text{m}/\text{min}$ and measured at $\sim 400 \text{ MHz}$.

Key words: piezoelectric properties, A&N epitaxial films, electromechanical coupling coefficient and growth defects.

*This work was supported in part by Contract No. F33615-72-C-1473, Air Force Materials Laboratory, Wright-Patterson Air Force Base, Ohio.

Introduction

Thin-film piezoelectric materials have been utilized for a number of years in the field of microwave acoustics. The earliest application of thin-film piezoelectrics was in the fabrication of bulk-wave transducers. Such materials as preferentially-oriented thin layers of CdS (1) and ZnO (2), with the c-axis parallel to the direction of propagation, were found adequate to efficiently generate bulk acoustic waves.

With the development of surface acoustic wave (SAW) devices (3, 4) a need was soon recognized for thin-film piezoelectric materials to provide a means of generation of surface acoustic waves on insulating low-loss acoustic materials. Again, preferentially-oriented ZnO was used. It was found, however, that preferentially-oriented ZnO thin films with the c-axis in the plane of the film showed extremely variable electromechanical coupling coefficients (5), and that to achieve optimum values of the coupling coefficient preferentially-oriented material showing a minimum of misoriented crystallites was necessary; at about the same time it was also shown that single-crystal ZnO films consistently yielded k^2 values approaching the theoretically predicted values (6). It is the intent of this paper to show that optimum acoustic properties can be obtained from single-crystal A&N films only if it is low in defect concentration.

A goal shared by many investigators of SAW devices is the development of epitaxial A&N on sapphire for potential use in a composite structure containing both a piezoelectric and a semiconducting material. This composite structure would contain a number of integrated circuits possessing both acoustic and semiconductor devices. A prime example of such a device is a SAW programmable tappable delay line where both an A&N delay line and silicon diodes and MOS devices are integrated on a single sapphire substrate. Further, such a composite structure is ideal for the fabrication of converters and correlators utilizing a multi-strip coupler (7) to produce an interaction of the piezoelectric field with the electronic charge carriers of a semiconductor. The application of this integrated technology awaits a method of growing epitaxial A&N of reproducible acoustic quality.

Experimental

The epitaxial films studied in these experiments were all grown by the CVD method described by Manasevit, Erdmann and Simpson (8). This method of AlN growth is accomplished by directing a mixture of trimethylaluminum (TMA) and ammonia onto a heated substrate in a flowing system. The postulated chemical reaction occurring is the pyrolytic decomposition of a trimethylaluminum-ammonia addition compound.

The TMA and ammonia were transported with ultrahigh-purity hydrogen to a sapphire substrate supported on a carbon susceptor coated with silicon carbide. The susceptor was heated inductively to growth temperatures ranging from 1200 to 1300C. Before growth, the polished sapphire substrates were subjected to a rigorous cleaning procedure. Substrates were cleaned by swabbing with TCE followed by soaking in a hot water detergent solution. The substrates were then thoroughly rinsed with deionized water followed by a 10% HCl solution. They were then placed in individual beakers, ultrasonically cleaned in acetone, and finally dipped in freon and blown dry in nitrogen gas. The cleaned substrate was placed on the susceptor and heated for five minutes at 1300C in hydrogen before growth was started. This final step before growth, was done to clean the reactor chamber and substrate of remaining foreign materials.

Sapphire bars approximately 0.6 mm thick with surface dimensions of 5 x 30 mm were used as substrates. These bars were fabricated with a strip of Si, coated with thermally-grown oxide, approximately 1 mm wide along one edge leaving a 4 mm strip of sapphire exposed. During growth of AlN, the strip of SiO₂/Si acted as a mask for the sapphire surface and allowed easy removal of a strip of AlN from the edge of the sample. The removed strip of AlN provided a step for accurate measurement of film thickness. The SiO₂/Si was removed by etching in a solution of 1:7 HF:HNO₃.

Measurement of the acoustic properties of the epitaxial AlN samples was accomplished using interdigital transducers (IDT) fabricated on the surface. In preparation for IDT fabrication, samples were polished and coated by

vacuum evaporation with approximately 800Å of aluminum. Fabrication of the IDTs followed the usual techniques of photolithography. Samples were fabricated typically with six or eight transducers forming adjacent rows. With this configuration of IDTs both reflective impedance and transmission measurements were made on different regions of the sample surface using a Hewlett-Packard network analyzer.

The acoustic measurements given in this paper were obtained from transducers designed at four different wave lengths (λ). The four transducers used were designed with equal lines and spaces with values of (λ) of 5.817, 14.15, 15.70 and 16.94 μm . The aperture of each transducer was 244, 333, 334, and 334 μm , respectively. These transducers produced acoustic signals in a frequency range of approximately 400 - 1000 mHz.

To establish the geometrical and electrical integrity of the transducers, measurement of capacitance C_T was made. Only IDTs showing values of capacitance within $\pm 10\%$ of the geometrically calculated value were used for acoustic measurements. After mounting the sample in a specially-constructed test jig, the transducer capacitance was series-inductively tuned at acoustic resonance. Reflective impedance and transmission measurements were then made on the sample using a network analyzer. These measurements yield data on the radiation resistance, resonance frequency, insertion loss, and phase shift as a function of frequency. Using these data, the coupling coefficient k^2 and phase velocity are calculated.

The electromechanical coupling coefficient is calculated using the equation $k^2 = F\pi^2 R_a f_0 C_T / 2N - 1$ (9), where R_a is the radiation resistance, f_0 is the acoustic resonance frequency, N is the number of finger pairs and F is the filling factor. For the purposes of these experiments, F was assumed to be unity. The phase velocity was calculated by the equation $V = \lambda f_0$. The k^2 data given in this paper were all obtained with $(11\bar{2}0)A\&N$ with propagation in the $[0001]$ direction of the $A\&N$ and in the $[011]$ direction of the Al_2O_3 .

Prior to acoustic measurements, the crystallographic properties of $A\&N$ samples were investigated using reflection electron diffraction. Only samples showing a pattern of individual spots indicating single-crystal structure

were used for acoustic measurements. Many of the samples investigated also showed Kikuchi lines in addition to the usual diffraction pattern. Some selected samples were also investigated by the Kossel x-ray technique. All samples investigated by this method showed extremely broadened reflection cones, interpreted to indicate highly-strained, single-crystal material.

Measurements of the electromechanical coupling coefficient (k^2) were made on a number of AlN samples, grown under various conditions, at different areas of the surface. Measurement of k^2 at different areas of the same sample, where the thickness h is equal, showed variations as large as a factor of three in some cases. Also, k^2 measured on different samples showed an unpredictable scatter over the range of h/λ from 0 to 0.6.

On the strength of these two observations, it was concluded that the epitaxial AlN contains a varying concentration of structural defects which directly affect the acoustic properties.

Variations noted in the measurement of k^2 on a single AlN film could not be correlated with patterns obtained from electron diffraction or Kossel x-ray observations. This fact is interpreted as showing that the defects producing the variation in k^2 are of a type and/or quantity which does not largely alter the single-crystal nature of the AlN layer and is not detectable by the usual electron or x-ray diffraction methods.

To study the relationship between the acoustic activity and structural quality of the epitaxial AlN layer, electron microscope observations of surface replicas were employed. Using standard methods of replication, surface structures of as-grown and etched epitaxial AlN were studied. The technique of replication was employed after it was found that adequate surface detail, such as growth facets or etch pits, was not resolvable using an optical microscope.

Figures 1 and 2 show electron micrographs of replicas of the as-grown surfaces of two different samples of AlN. The replicas of these surfaces were taken at the region where interdigital transducers had been fabricated. The

A&N sample shown in Figure 1 had an electromechanical coupling coefficient of 0.40%. This sample shows well-aligned facets over the entire area occupied by the transducer. Growth facets having a well-aligned structure as shown in Figure 1, are typical of single-crystal material. The alignment of the principal growth facets is along the c-axis, as determined by x-ray diffraction analysis.

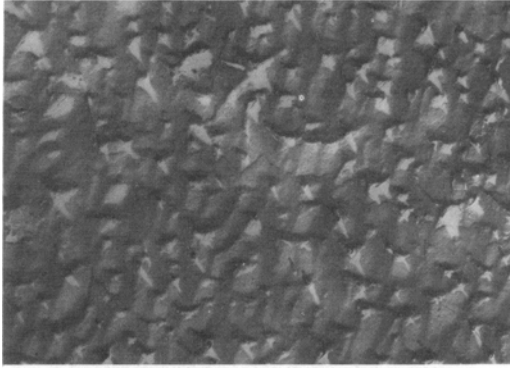


Figure 1. Electron Micrograph of As-grown A&N Surface Replica, k^2 value = 0.4%, magnification 9750X.

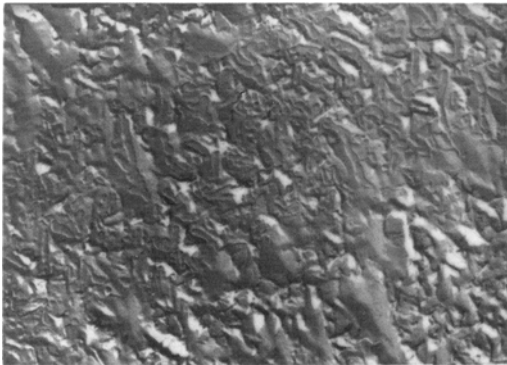


Figure 2. Electron Micrograph of As-grown A&N Surface Replica, k^2 value $\cong 0$ magnification 9750X.

Figure 2 shows an electron micrograph of a replica of an AlN surface with a k^2 of approximately zero. It is seen in this figure that the as-grown facets are not well ordered, although they do have a ridged structure with general ordering in the c-axis direction.

Figures 3 and 4 show electron micrographs of replicas of an etched surface of two different areas of a single sample where transducers were located and different k^2 values were obtained. The AlN surface was etched with a 20% solution of sodium hydroxide. The etching time for this sample was approximately 10 minutes which removed approximately 0.5 μm of AlN from the surface. The k^2 values measured at 400 MHz for the sample shown in Figures 3 and 4 were 0.25% and 0.14%, respectively. The thickness-to-wavelength ratio h/λ is 0.11 at both transducer locations. In Figure 3, well-ordered, long straight facets are observed aligned along the c-axis, with only a few defects interrupting the pattern. In contrast, Figure 4 shows a surface structure with all facets generally aligned along the c-axis but with numerous interruptions of the pattern by surface defects.

These data clearly show that larger k^2 values are obtained from samples showing greater geometrical perfection of the facets independent of whether they are observed on as-grown or etched surfaces.

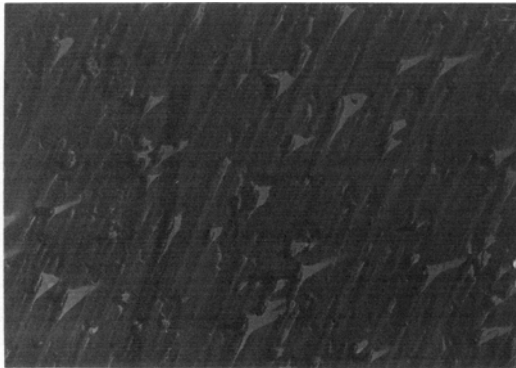


Figure 3. Electron Micrograph of Etched AlN Surface, $k^2 = 0.25\%$, magnification 9750X.

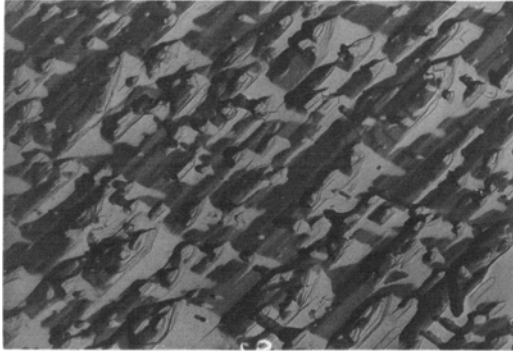


Figure 4. Electron Micrograph of Etched AlN Surface, $k^2 = 0.14\%$, magnification 9750X.

Discussion

The data of Figure 5 represents only the maximum value of k^2 obtained from 71 different AlN samples. On each of these samples, from one to as high as six separate values of k^2 were determined. These samples ranged in thickness from about $1 \mu\text{m}$ to $6 \mu\text{m}$ and were measured using the transducers described which produced signals from approximately 400 to 1000 mHz. Thickness measurements made at each transducer site were used to compute h/λ values from .01 to 0.2. A plot of all k^2 values versus h/λ showed a widely scattered array of points. The plot of Figure 5 was constructed by selecting only the maximum values of k^2 at any particular h/λ value on the assumption that the maximum value approaches the intrinsic k^2 for high perfection single crystalline AlN. Included in Figure 5, are data published by O'Clock and Duffy (10). Combining these data with those of the present work, the possibility of the existence of an auxiliary maximum in k^2 at $h/\lambda \approx 0.05$ followed by a minimum value at $h/\lambda \approx 0.07$ arises.

Theoretical calculations (11, 12) of the dispersion characteristics of other layered systems, such as ZnO on sapphire, have predicted the occurrence of an auxiliary maximum in the k^2 -versus- h/λ data. Experimental data (6) on epitaxial $(11\bar{2}0)\text{ZnO}$, which is crystallographically isomorphic with epitaxial AlN, grown on $(01\bar{1}2)$ sapphire,

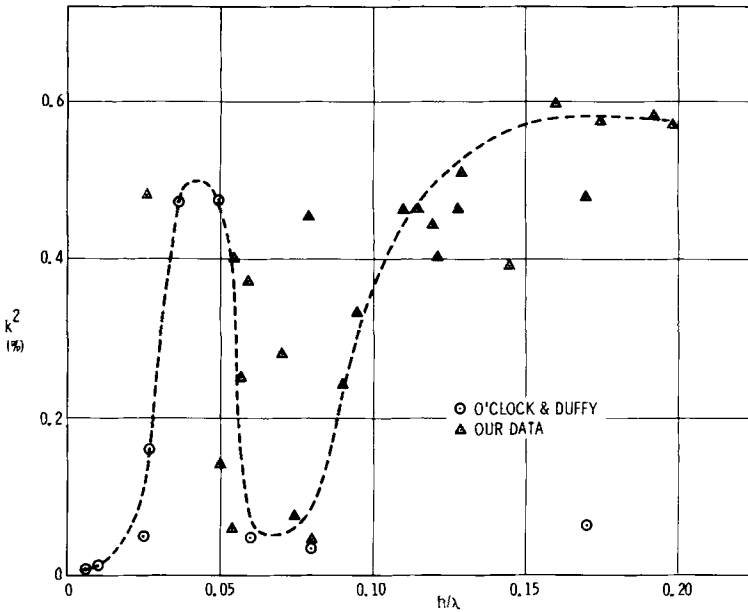


Figure 5. Plot of Maximum Values of k^2 Measured on Samples in the Range of h/λ from 0 to 0.2.

also show an auxiliary maximum at $h/\lambda = 0.12$. Although there is good evidence given in Figure 5 for the existence of an auxiliary maximum, as shown by the dashed curve, there is sufficient experimental error produced by the variation in the quality of the samples to make this conclusion somewhat speculative at this time.

The experimental data showed that k^2 measured on epitaxial layers 2 to 3 μm thick at a frequency of 400 MHz ($h/\lambda \sim 0.13$ to ~ 0.2) typically were the highest values. Samples 2 to 3 μm thick measured at approximately 500 MHz usually showed some degradation in k^2 with respect to the values obtained at 400 MHz. When samples approximately 1 μm ($h/\lambda \cong 0.22$) thick were measured at a frequency of 1080 MHz, a degradation of k^2 to 0.1% was also noted. These data, yet unexplained, indicate that the defect existing in the AlN layer may produce a frequency-dependent degradation of k^2 .

Samples 3 to 6 μm thick have also been investigated. Again, a wide variation in k^2 was observed, presumably caused by the same factors producing the observed variations in samples of 2 to 3 μm thickness. Although there were fewer samples measured in this thickness range than in the 2 to 3 μm range, the overall variation in k^2 is comparable.

Conclusions

The random variations experimentally observed in k^2 at different areas of the same sample are more reasonably explained by postulating a random variation of the concentration of growth defects than by a uniform stress produced by the thermal mismatch between layer and substrate.

This postulate of a variable defect concentration is further strengthened by the surface replicas of different regions of the same sample showing wide differences in the geometrical ordering of the growth facets.

The origin of the defects can be attributed to many possible factors, including variable crystalline properties of the sapphire substrate, local fluctuation in the gas ambient conditions during growth, and local fluctuation in the temperature of the substrate during growth. Although the relationship between the coupling coefficient k^2 and the type and concentration of defect producing degradation in k^2 has not been established, the experimental data clearly show that a relationship exists. The type of defects causing degradation of k^2 probably include such crystallographic imperfections as random inclusion of polycrystalline particles, grain boundaries, and c-axis inversion twinning.

To explain the degradation of k^2 , a physical mechanism involving inversion twinning is easily postulated. In brief, a total or partial cancellation of the piezoelectric strain produced by an electric field would result at a region of the A&N under the IDT where c-axis inversion exists. Unfortunately, inversion twinning is extremely difficult to identify by either x-ray or electron diffraction techniques; consequently, any systematic investigation of the defects in epitaxial A&N should include either

electron microscopic examinations of surface replicas such as given in this paper or Scanning Electron Microscope observations of as-grown and etched surfaces to delineate and identify the entire range of detectable surface defects, and also appropriate structural analyses by x-ray techniques.

Acknowledgments

The authors wish to acknowledge the electron diffraction analysis and replication work on the samples of A&N done by J. P. Kenty and R. E. Johnson, the transducer fabrication done by L. Dyal, and the advice and suggestions given by A. J. Hughes, H. M. Manasevit and R. P. Ruth.

References

1. N. F. Foster, Trans. AIME 230, 1503 (1964).
2. N. F. Foster and G. A. Rozgonyi, Appl. Phys. Lett. 8, 221 (1966).
3. F. S. Hickernell, IEEE Ultrasonic Symposium, 1971, Miami Beach, Paper P-1.
4. C. B. Wellingham, M. G. Holland, M. B. Schulz, and J. H. Matsinger, ibid., Paper P-3.
5. A. J. Bahr, R. E. Lee, F. S. Hickernell, C. B. Wellingham, and T. M. Reeder, IEEE Ultrasonics Symposium Proceedings, Oct. 1972, Boston, page 203, IEEE Cat. No. 72CH0708-850.
6. F. Pizzarello, J. Appl. Phys. 43, 3627 (1972).
7. F. G. Marshall and E. G. S. Paige, Electronics Lett. 7, 460 (1971).
8. H. M. Manasevit, F. M. Erdmann, and W. I. Simpson, J. Electrochem. Soc. 118, 1864 (1971).
9. W. R. Smith, H. M. Gerard, J. H. Collins, T. M. Reeder, and H. J. Shaw, IEEE Trans. Vol. MTT-17, 856 (1969).

10. G. D. O'Clock, Jr., and M. T. Duffy, Appl. Phys. Lett. 23, 55 (1973).
11. W. R. Smith, J. Appl. Phys. 42, 3016 (1971).
12. K. Lakin and D. Penunuri, IEEE Symposium, Miami Beach, 1971, Paper D-7 (unpublished).